Smart Materials and Structures

A 3D Multidirectional Piezoelectric Energy Harvester using Rope-Driven Mechanism for Low Frequency and Ultralow Intensity Vibration Environment

To cite this article before publication: Jinhui Zhang *et al* 2021 *Smart Mater. Struct.* in press https://doi.org/10.1088/1361-665X/ac3f77

A 3D Multidirectional Piezoelectric Energy Harvester using Rope-Driven Mechanism for Low Frequency and Ultralow Intensity Vibration Environment

Jinhui Zhang[a], Maoyu Lin[a, b], Wei Zhou[a], Lihua Tang[c] and Lifeng Qin[a, b, *]

[a] Department of Mechanical and Electrical Engineering, Xiamen University, Xiamen 361102, China
[b] Shenzhen Research Institute of Xiamen University, Shenzhen 518000, China
[c] Department of Mechanical Engineering, University of Auckland, Auckland 1010, New Zealand
[*] Correspondence: liq@xmu.edu.cn

Abstract

Though numerous piezoelectric vibration energy harvesters (PVEHs) have been designed and investigated to provide power supply for wireless sensors or wearable devices, it remains a challenge for traditional PVEHs to work effectively in an environment of low frequency, low acceleration and multidirectional vibrations. This work presents a PVEH using a low-frequency energy-capturing resonant system formed by a rolling ball in a hemispherical shell and driven by a rope. Due to the symmetry of the sphere, the ball can be excited at multiple directions in 3D space, and the piezoelectric beam can be pulled by the ball through a rope in multiple directions. Thus, the efficient multidirectional energy harvesting under low frequency (< 10 Hz) and ultralow intensity (< 0.1 *g*) vibrations could be realized. A mass-spring-damper equivalent model was built to understand the operation mechanism of the proposed PVEH. The results show that the proposed PVEH has a potential to collect energy in any direction in 3D space, and could achieve a good angle bandwidth with 360° for φ and 240° for β under the excitation of a = 0.04 *g*, f = 6.8 Hz with the acceleration $\vec{a}(a,\beta,\varphi)$ defined in the spherical coordinate system. The developed PVEH can generate 6.5 μW under a low-intensity excitation (0.03 *g*), and the normalized power density can reach 22.63 μW/(cm^3*g*^{2}Hz). Moreover, the minimum start-up acceleration analysis of the proposed PVEH indicates that the PVEH can capture multidirectional energy from vibrations as low as 0.01 *g*. In addition, both simulation and experimental study on rope redundancy and ball mass show that they can be used to adjust the device performance easily without structure re-fabrication. Overall, this study demonstrates a new mechanism that could effectively harvest low frequency, ultralow intensity and multidirectional vibration energy.

Keywords: piezoelectric vibration energy harvester, low frequency, ultralow intensity, multidirectional

1. Introduction

Piezoelectric vibration energy harvesting technique is highlighted as an effective method for achieving a self-powered wireless sensor networks (WSN) because piezoelectric material can directly convert mechanical vibration into electrical energy with a high power density and the corresponding device can be created using a simple structure [1–8]. A typical piezoelectric vibration energy harvester (PVEH) can be constructed by a cantilever beam structure with a proof mass attached at the free end and piezoelectric material boned on a substrate near its root [9]. Such devices only work effectively when excitation is applied perpendicular to the beam with a decent acceleration level and at a relatively high frequency matching the natural frequency of the beam [10]. In practice, low frequency (< 10 Hz) [11–14], ultralow intensity (< 0.1 *g*) [11,15–18] and multidirectional kinetic energy [19] are ubiquitous in the environment mainly in the form of vibration (shown in Table 1). Hence, PVEHs that can capture energy effectively in a low frequency, ultralow intensity and multidirectional vibration environment is necessary for applications of some electronics.

Table 1. Common low frequency, ultralow acceleration vibration sources [11,12,15–18,20–22].

Vibration sources	Frequency (Hz)	Maximum acceleration (*g*)
Human walking	2–3	0.2–0.3
Ocean platform	0.35	0.001–0.017
High building vibration caused by strong wind	0.1–1	0.002–0.043
Bridge vibration caused by car	3.3–15.9	0.006–0.022
Houses near the road	8–20	0.0002–0.0012

In terms of low frequency vibration energy harvesting, one early and direct method is to decrease the spring stiffness of the cantilever beam, such as increasing its length by adopting a curved beam [23–25] or decreasing its Young's modulus by using polymeric substrates [26,27]. Later, one more efficient and main strategy is to introduce a frequency up-conversion (FUC) mechanism in which a low frequency structure is used to capture low frequency vibration energy and triggers high frequency oscillations of a piezoelectric beam through a contact [14,24,28–33] or non-contact force [5,34–39], consequently realizing a high mechanical-electrical conversion under low frequency vibration.

For achieving multidirectional energy harvesting, one straight forward strategy is to increase the piezoelectric cantilever beams distributed in different directions [40–43]. For example, Su et al. [40] proposed a piezoelectric energy harvester consisting of a main beam, an auxiliary beam,

and a spring-mass system, sensitive to Z, Y, X axis excitation respectively. Nonlinear force was introduced to couple these three sub-systems by setting permanent magnets at the end of these three subsystems, thus the harvester could capture tri-directional vibration energy. Chen et al. [41] represented a dandelion-like multidirectional generator consisted of thirteen piezoelectric cantilever beams, multi-faceted support body and upright column, where each beam was fixed on the multi-faceted support body in different directions to sense to excitation in thirteen directions respectively. While the disadvantage of this method is low volume efficiency because of the fact that each piezoelectric cantilever beam can vibrate effectively in a single direction. To address this problem, method based on the specific design of beam structure or material choice [44–52] was proposed. For example, Wang et al. [50] presented a two-dimensional PVEH using a flexible cylindrical rod instead of the straight beam with radially distributed piezoelectric array. A concept of angle bandwidth (the range of angle corresponding to the output of the PVEH $> 1/\sqrt{2}\ V_{max}$) was first used to describe the harvester's multidirectional performance, and this device showed an angle bandwidth of 106.3° in two-dimensional plane.

Although a lot of PVEHs have been designed for low frequency or multidirectional vibration energy harvesting as mentioned above, simultaneously achieving low frequency, ultralow intensity, and multidirectional vibration energy harvesting is still a challenge, especially in 3D space, and there are a very few related reports so far. Xu et al. [53] reported a pendulum-based harvester where the fixed proof-mass in a typical piezoelectric cantilever was replaced with a pendulum, resulting in a capability of harvesting multidirectional vibration energy with characteristics of low frequency and low intensity. Further, to enhance the energy harvesting output performance, Wu et al. [13] presented a similar pendulum based PVEH by replacing the straight piezoelectric beam with a series of binder clips attached with piezoelectric materials. However, for pendulum-based PVEHs, due to its resonant characterise of pendulum, it requires a big mass ball and long pendulum spring for low frequency energy harvesting, thus a relatively heavy structure and large space for ball's movement. Moreover, when the heavy ball is not perpendicular to piezoelectric beam during the movement of ball, it will produce a twist on piezoelectric beam, which will affect the long-term reliability of the device. Our prior work [54] proposed a new PVEH comprising a cylindrical container with a certain liquid, a piezoelectric cantilever beam, floater-lever arrays and ropes. The liquid was used as an energy-capturing medium to realize multidirectional vibration energy harvesting under a low frequency, low intensity vibration. Although a good angle bandwidth of 360° in horizontal plane was achieved, it has a non-ideal output in vertical plane. Therefore, until

now, there have not been significant previous studies on the developing PVEHs in 3D space for low frequency and ultralow intensity vibration energy harvesting. On the other hand, in a real world environment, ambient excitations may come from various directions such as human motions and ocean platform [12,22], it is desirable to present a 3D multidirectional energy harvester to maximize the harvested energy.

In this work, we propose a new 3D multidirectional PVEH based on a rope-driven mechanism for effective energy harvesting from a low frequency (< 10 Hz), ultralow intensity (< 0.1 *g*) and multidirectional vibration environment. The PVEH consists of a rolling ball in a hemispherical shell, a piezoelectric beam and a rope. The ball placed in the shell in nature forms a low-frequency energy-capturing resonant system, where the ball can be excited at multiple directions in 3D space due to the symmetry of the sphere. The piezoelectric beam can obtain the energy from the ball with the rope connection, and the cyclic deformation of the piezoelectric layer on the beam will be converted into electricity based on the direct piezoelectric effect. The experimental results manifest the promising potential of the proposed approach for capturing energy existing in practical vibration environments as a power source for wireless sensors. The originality and advantages of our proposed PVEH are summarized as follows.

(1) Unlike traditional beam based low frequency PVEHs, a new low frequency PVEH based on a rope-driven mechanism using a spherical ball placed in a hemispherical shell as a low-frequency energy-capturing resonant medium is first proposed, which has the capable of capturing mechanical energy in arbitrary direction in 3D space.

(2) A novel mechanical energy transformation structure, comprising a catheter, a rope and a spherical ball, is proposed. It can transfer arbitrary direction excitations to one direction perpendicular to the beam, which can avoid beam twisting, and realize a good angle bandwidth in 3D space.

(3) The new PVEH can achieve a large angle bandwidth of 360° in horizontal plane and 240° in vertical plane under a low frequency of 6.8Hz and an ultralow intensity of 0.04 *g*. Meanwhile, a comparable normalized power density of 22.63 $\mu W/(cm^3 g^2 Hz)$ is also realized compared with the existing multidirectional PVEHs. Moreover, the PVEH's adjustable performance can be realized by controlling rope redundancy or ball mass.

The rest of the paper is organized as follows. Section 2 describes the working principle of the proposed PVEH; Section 3 presents the characterization and experimental setup of the PVEH; Section 4 gives an experimental results of the device's energy harvesting performance subjected

to low frequency, ultralow intensity and 3D-multidirectional vibrations and discussed the strategy to adjust the performance by tuning rope redundancy and ball mass; Main findings and conclusive remarks are summarized in Section 5.

2. Working Principle

Fig. 1 shows the proposed multidirectional PVEH composed of a hemispherical shell, a spherical ball which can roll inside the shell without slipping, a piezoelectric energy generating beam and a rope through a catheter connecting the beam and the spherical ball. The ball and the shell in nature form a low-frequency resonant system, where the ball can produce significant rolling subjected to excitation close to the resonant frequency of this system to capture kinetic energy. Due to the symmetry of the sphere, the ball can be excited at multiple directions in 3D space. The ball will roll inside the shell violently and exceed the rope redundancy (defined as rope length minus the distance from beam end *A* to connecting point *C*) around the resonant frequency of the low-frequency energy-capturing system. The piezoelectric beam would then be pulled by the tightened rope through the catheter, where the force from different directions can be changed to one direction aligned with beam bending motion to avoid beam twisting. Because the ball rolls back and forth, during one vibration cycle, the beam is pulled twice by the ball. Meanwhile, the cyclic deformation of the piezoelectric layer on the beam will be converted into electricity via the direct piezoelectric effect. The typical voltage output with a resistive load of 300 kΩ of the proposed PVEH is shown in Fig. 2.

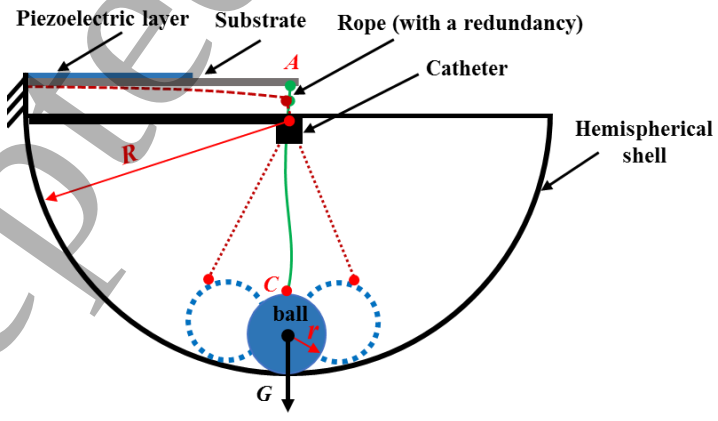

Figure 1. Schematic of the 3D multidirectional PVEH.

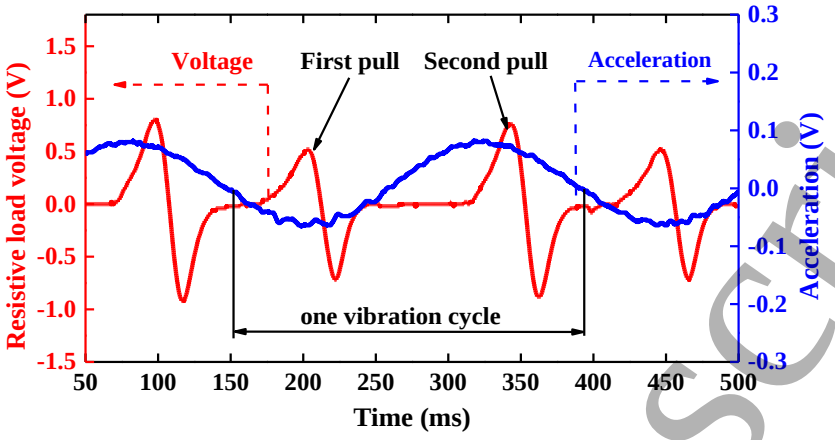

Figure 2. Typical voltage output across a resistive load of the 3D multidirectional PVEH around resonance.

3. Characterization and Experimental Setup

3.1 Resonant Frequency of Ball Rolling in Shell

The proposed PVEH adopts the ball rolling without slipping in a spherical shell as a resonant energy-capturing system that can operate effectively in a low frequency, low intensity and multidirectional excitation scenario.

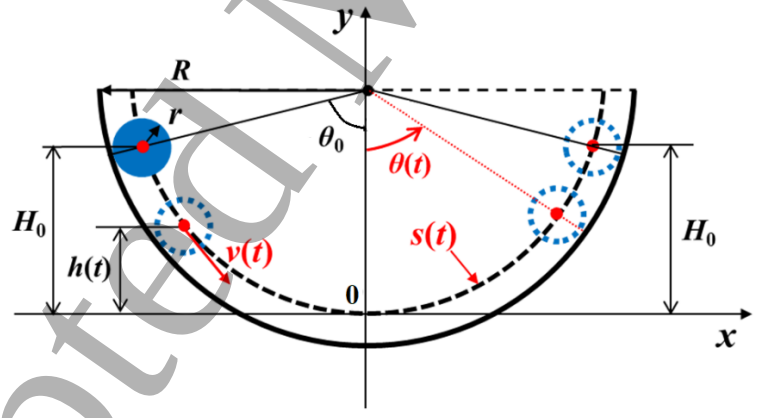

Figure 3. Schematic of the low frequency resonant energy-capturing system formed by the ball rolling in the spherical shell

For simplifying the analysis, the damping is assumed to be negligible as the ball without rope connection. When the ball is released from an initial height H_0 (Fig. 3), the energy is conserved, that is

$$E_k + E_p = mgH_0 \tag{1}$$

where E_k is the kinetic energy

$$E_k = \frac{1}{2}\left(I_c + mr^2\right)\left(\frac{R-r}{r}\dot{\theta}(t)\right)^2 \tag{2}$$

and E_p is the potential energy

$$E_p = mg\left(R-r\right)\left(1-\cos\theta(t)\right) \tag{3}$$

where $\theta(t)$ is the angular coordinate defining the position of ball at time t. $I_c = 2/5\ mr^2$ is the moment of inertia of the rolling ball about its centre of mass. Substituting Eqs. (2) and (3) into Eq. (1), and differentiating Eq. (1) with respect to t, we have

$$\frac{7}{5}(R-r)\ddot{\theta}(t) + g\sin\theta(t) = 0 \tag{4}$$

For small vibration $\theta(t)$, Eq. (4) can be linearized as

$$\frac{7}{5}(R-r)\ddot{\theta}(t) + g\theta(t) = 0 \tag{5}$$

and the natural frequency f of the linearized system is

$$f = \frac{1}{2\pi}\sqrt{\frac{5g}{7(R-r)}} \tag{6}$$

In case of large $\theta(t)$, numerical method should be used to calculate the resonant frequency of the system. The resonant frequency of this system can be determined by measuring the time of the ball complete half vibration cycle in the shell when released from an initial height H_0 with the initial angle θ_0 ($t = 0$) (Fig. 3). Since $v(t) = (R-r)\dot{\theta}(t)$, Eq. (1) can be rewritten as

$$\frac{1}{2}I_c\left(\frac{v(t)}{r}\right)^2 + \frac{1}{2}mv(t)^2 + mgh(t) = mgH_0 \tag{7}$$

Rearranging Eq. (7) gives the velocity of the ball

$$v(t) = \sqrt{\frac{10}{7}g\left(H_0 - h(t)\right)} \tag{8}$$

The resonant frequency f of the low-frequency energy-capturing system can be predicted by calculating the time of completing half cycle of the ball rolling back and forth numerically, that is

$$f = \frac{1}{2T} = \frac{1}{2\int_{-\theta_0}^{\theta_0}\frac{ds(t)}{v(t)}} = \frac{1}{2}\frac{1}{\int_{-\theta_0}^{\theta_0}\frac{(R-r)d\theta(t)}{\sqrt{\frac{10}{7}g\left(H_0-(R-r)\left(1-\cos\theta(t)\right)\right)}}} \tag{9}$$

where $s(t)$ is arc displacement of the ball centroid.

Fig. 4 shows the results based on Eqs. (6) and (9) in the case of $R = 27.8$ mm, $r = 9$ mm, $\theta_0 =$

0~90°. It can be seen that the resonant frequency predicted by these two methods is consistent for small θ_0 and the discrepancy increases with the increase of θ_0. Hence, the numerical method with Eq. (9) should be used to accurately predict the resonant frequency of the system, which is confirmed by experimental results shown in Table 2 and Table 3. In this experiment, the resonant frequency was determined by the maximum response subjected to the harmonic excitation with an acceleration amplitude of 0.03 g and varying frequencies. The response was recorded by a high-speed camera, and the angles were measured by a machine vision software shown in Figs. 5 and 6. It is worth mentioning that the maximum angles (θ_{max}) obtained in experiment when the system resonates is used to calculate the theoretical resonant frequency by setting θ_0 to be θ_{max} in Eq. (9).

Moreover, from Eqs. (6) and (9), it can be found that the resonant frequency of the low-frequency energy-capturing system could be reduced by increasing the shell radius or decreasing the ball radius, which is helpful for the PVEH achieving low-frequency energy harvesting. Based on the theoretical and experimental results mentioned above, a low frequency resonant energy-capturing system (R = 27.8 mm, r = 9 mm) is designed to investigate the performance of the proposed PVEH.

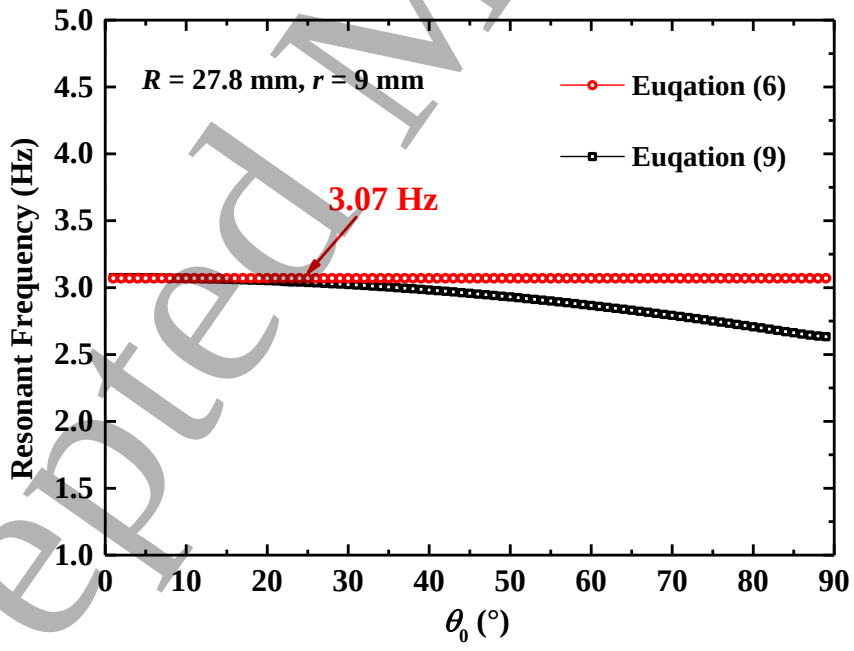

Figure 4. Resonant frequency of the energy-capturing system as a function of the initial angle θ_0 with a ball radius of 9 mm and a shell radius of 27.8 mm.

Table 2. Comparison of the theoretical and experimental results of resonant frequency of the energy-capturing system with different ball radii.

r (mm)	R (mm)	θ_{max} in experiment at resonance (°)	Experimental resonant frequency (Hz)	Theoretical resonant frequency (Hz)	
				Equation (9)	Equation (6)
4	27.8	26.8±1	2.70	2.70	2.73
9	27.8	26.1±1	3.04	3.04	3.07
11	27.8	23.1±1	3.20	3.22	3.25

Table 3. Comparison of the theoretical and experimental results of resonant frequency of the energy-capturing system with different shell radii.

r (mm)	R (mm)	θ_{max} in experiment at resonance **(°)**	Experimental resonant frequency (Hz)	Theoretical resonant frequency (Hz)	
				Equation (9)	Equation (6)
9	22.5	23.5±1	3.60	3.60	3.62
9	27.8	26.1±1	3.04	3.04	3.07
9	32.2	20.4±1	2.74	2.75	2.76

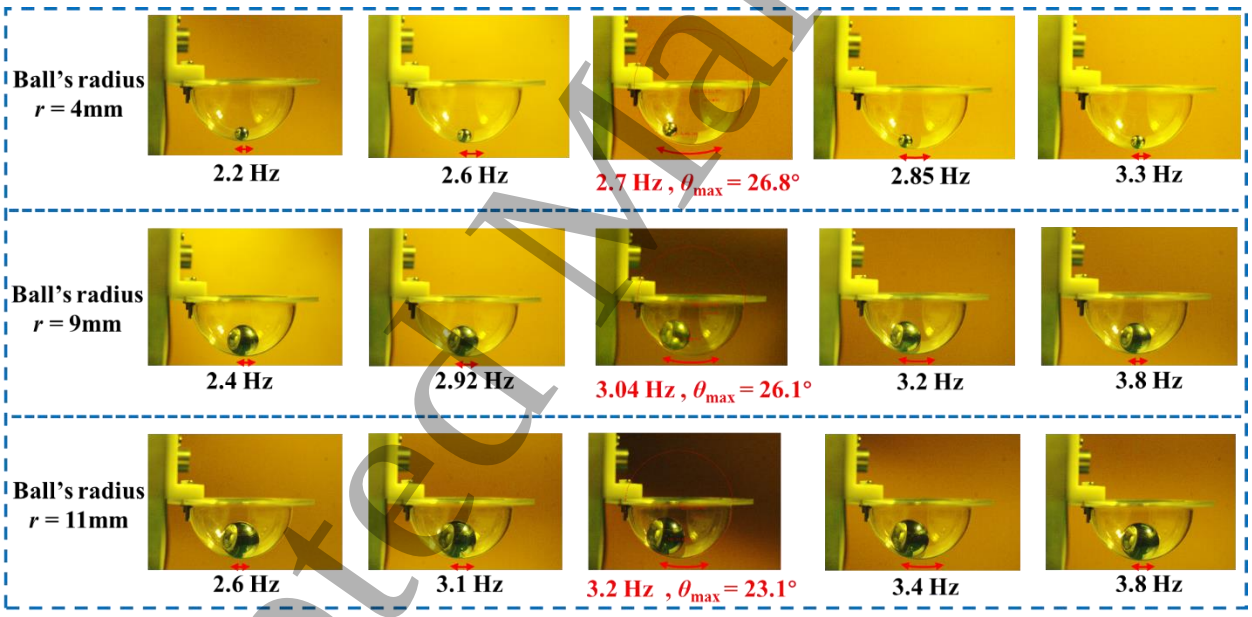

Figure 5. High speed camera recorded responses of the energy-capturing system at varying frequencies around resonance with different ball radii.

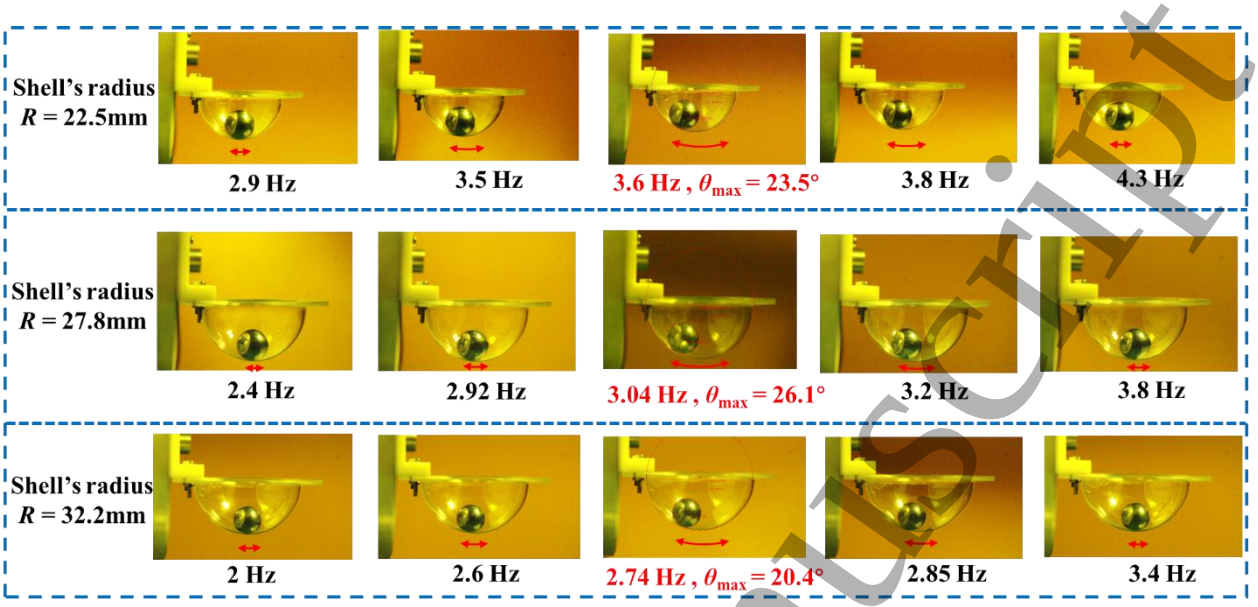

Figure 6. High speed camera recorded responses of the energy-capturing system at varying frequencies around resonance with different shell radii.

3.2 Modeling of the proposed PVEH

As the ball with rope connection, different from the case of the ball without rope connection, the ball movement can be seen as rolling in the hemispherical shell with a small angle. Fig. 7 illustrates a mass-spring-damper equivalent model of the proposed PVEH with a rope connecting the beam and ball. As shown in Fig. 7(a), the equivalent schematic model comprises of a ball and shell as a a low-frequency energy-capturing system with a ball radius r and shell radius R, and a piezoelectric beam as generator with a damping coefficient c, stiffness k, and proof mass m. A rope with stiffness k_0 is used to connect the ball and beam with an initial length l_0. The connection point of rope with piezoelectric beam and ball is A and C respectively. Assuming the connection point A is through the shell center, the rope redundancy δ can be expressed by:

$$\delta = l_0 - (R - 2r) \tag{10}$$

When the proposed PVEH system is excited by a base excitation $z(t)$, which has an angle β with horizontal plane, as shown in Fig. 7(b), the ball starts to roll with a rotation angle θ and self-rolling angle α, where the beam wouldn't be pulled by the ball as the rope relaxing (phase 1). As the ball continues to roll shown in Fig. 7(c), the rope is tightened, and the rolling ball pulls the beam through the rope. The beam suffers from a tension T with a downward displacement x by the rolling ball (phase 2), and the rope is stretched with a length Δl.

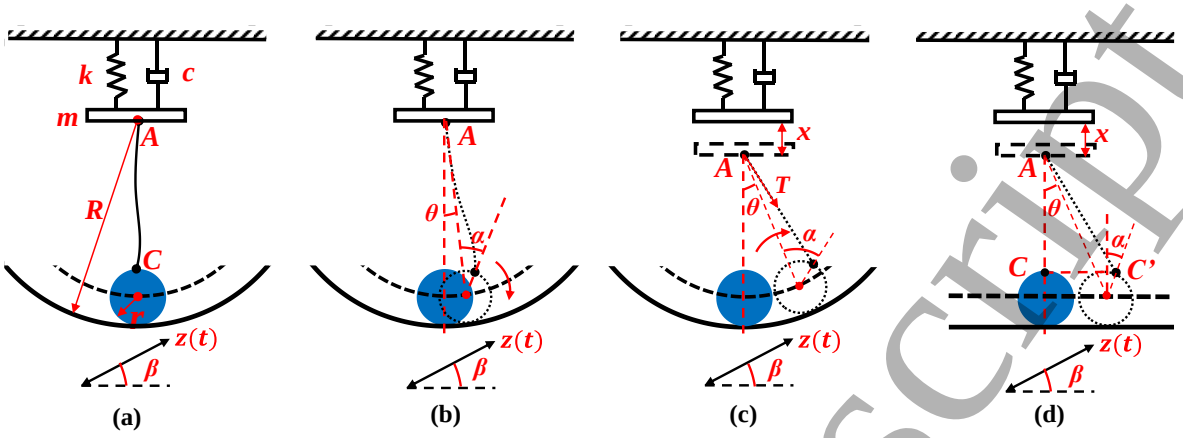

Figure 7. Schematic model and operation mechanism of the proposed PVEH system.

According to the equivalent schematic models and operating mechanism of the proposed PVEH, the motion equations of the rolling ball (θ) and beam (x) can be written as:

$$J_c\ddot{\alpha} = \begin{cases} -Mrg\sin\theta - c_1\dot{\theta} - Mr\ddot{z}\cos\beta\cos\theta & (\Delta l < 0),\ phase\ 1 \\ -Mrg\sin\theta - c_1\dot{\theta} - Mr\ddot{z}\cos\beta\cos\theta - \dfrac{TRr\sin(\theta+\alpha)}{R\text{-}r} & (\Delta l \geq 0),\ phase\ 2 \end{cases} \tag{11}$$

$$m\ddot{x} = \begin{cases} -kx - c\dot{x} + m\ddot{z}\sin\beta & (\Delta l < 0),\ phase\ 1 \\ -kx - c\dot{x} + m\ddot{z}\sin\beta + T\cos\theta & (\Delta l \geq 0),\ phase\ 2 \end{cases} \tag{12}$$

where J_c is the moment of inertia of the rolling ball about its contact point with shell, g is the acceleration of gravity, M and c_1 are the ball mass and damping characteristics, m and c are the beam mass and damping characteristics.

For small rotation angle θ, Fig. 7(c) can be repainted as Fig. 7(d). From Fig. 7(d), we can get:

$$AC'^2 = AC^2 + CC'^2 \tag{13}$$

Considering the condition $AC' = l_0+\Delta l$, $AC = R\text{-}2r\text{-}x$, $CC' \approx \theta R+\alpha r$, and $l_0 = R\text{-}2r+\delta$, $\theta R = \alpha r$, we can find the expression of x:

$$x = (R-2r) - \sqrt{(R-2r+\delta+\Delta l)^2 - 4R^2\theta^2} \approx \frac{2R^2\theta^2}{R-2r+\delta+\Delta l} - \delta - \Delta l \tag{14}$$

Due to Δl is much smaller than $R\text{-}2r+\delta$, the stretch length of rope can be expressed approximately by:

$$\Delta l \approx \frac{2R^2\theta^2}{R-2r+\delta} - \delta - x \tag{15}$$

Here, the rope is assumed to be a spring without damping, thus tension $T = k_0\Delta l$. By substituting the expression of T, Eqs. (11) and (12) can be rearranged as follows:

$$J_c \frac{R}{r}\ddot{\theta}+Mrg\theta+c_1\dot{\theta}=\begin{cases}-Mr\ddot{z}\cos\beta & (\Delta l<0),\ phase\ 1\\ -Mr\ddot{z}\cos\beta-k_0(\dfrac{2R^2\theta^2}{R-2r+\delta}-\delta-x)\dfrac{R(R+r)}{R-r}\theta & (\Delta l\geq 0),\ phase\ 2\end{cases} \quad (16)$$

$$m\ddot{x}+kx+c\dot{x}=\begin{cases}+m\ddot{z}\sin\beta & (\Delta l<0),\ phase\ 1\\ +m\ddot{z}\sin\beta+k_0(\dfrac{2R^2\theta^2}{R-2r+\delta}-\delta-x) & (\Delta l\geq 0),\ phase\ 2\end{cases} \quad (17)$$

Thus, the displacement of the piezoelectric beam versus the excitation frequency can be numerically derived based on Eqs. (16) and (17).

3.3 Experimental Setup

To describe the direction of excitation acceleration clearly, a spherical coordinate system is established to define the direction of acceleration from the vibration environment (Fig. 8). The *X*-direction is along the beam length, *Y*-direction is along the beam width and the direction of gravity (*G*) is in the opposite *Z*-direction. An arbitrary excitation acceleration $\vec{a}(a,\beta,\varphi)$ is described in the spherical coordinate system, where *a* is the magnitude of acceleration, β is the elevation angle, and φ is the azimuth angle. During the experiments, because the sphere is an axisymmetric geometry, we take angle β in a range of -90º–90º, and φ in a range of 0º–360º to study the multidirectional energy harvesting performance of the proposed PVEH in 3D space.

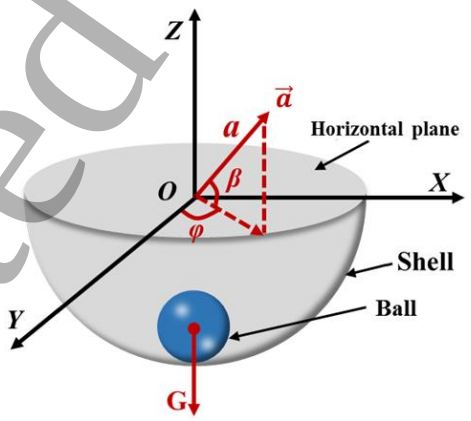

Figure 8. Excitation acceleration in the spherical coordinate system.

Fig. 9 depicts a schematic of the experimental setup for characterizing the proposed 3D multidirectional PVEH. A signal generator and a power amplifier are used to control the vibration frequency and amplitude of the shaker, which is monitored by an accelerometer. The detailed parameters of the fabricated 3D multidirectional PVEH prototype are shown in Table 4, where the

piezoelectric beam has a natural frequency of 211.2 Hz. The prototype is mounted on customized fixtures with different angles to adjust the elevation angle β from -90º to 90º. Moreover, a small fixture tuning platform with a precision of 0.01 mm is used to finely control the rope redundancy during the experiments. A lead zirconate titanate (PZT) generating beam is connected with a resistance box. Meanwhile, a data acquisition (DAQ) module is used to record the root mean square (RMS) voltage across the resistive load.

Table 4. Parameters of the 3D multidirectional PVEH in experiment and simulation.

Parameter	Substrate	PZT 5A	ball	Shell
Length (mm)	30.0	12.0	/	/
Width (mm)	26.0	26.0	/	/
Thickness (mm)	0.20	0.13	/	/
Piezoelectric constant d_{31} (10^{-12} C/N)	/	-190	/	/
Relative dielectric constant ε^{T}_{33}	/	1800	/	/
Mass (gram)	/	/	10 - 46	/
Radius (mm)	/	/	9	27.8
Damping ratio	0.02		0.08	
Frequency (Hz)	211.2		3.04	

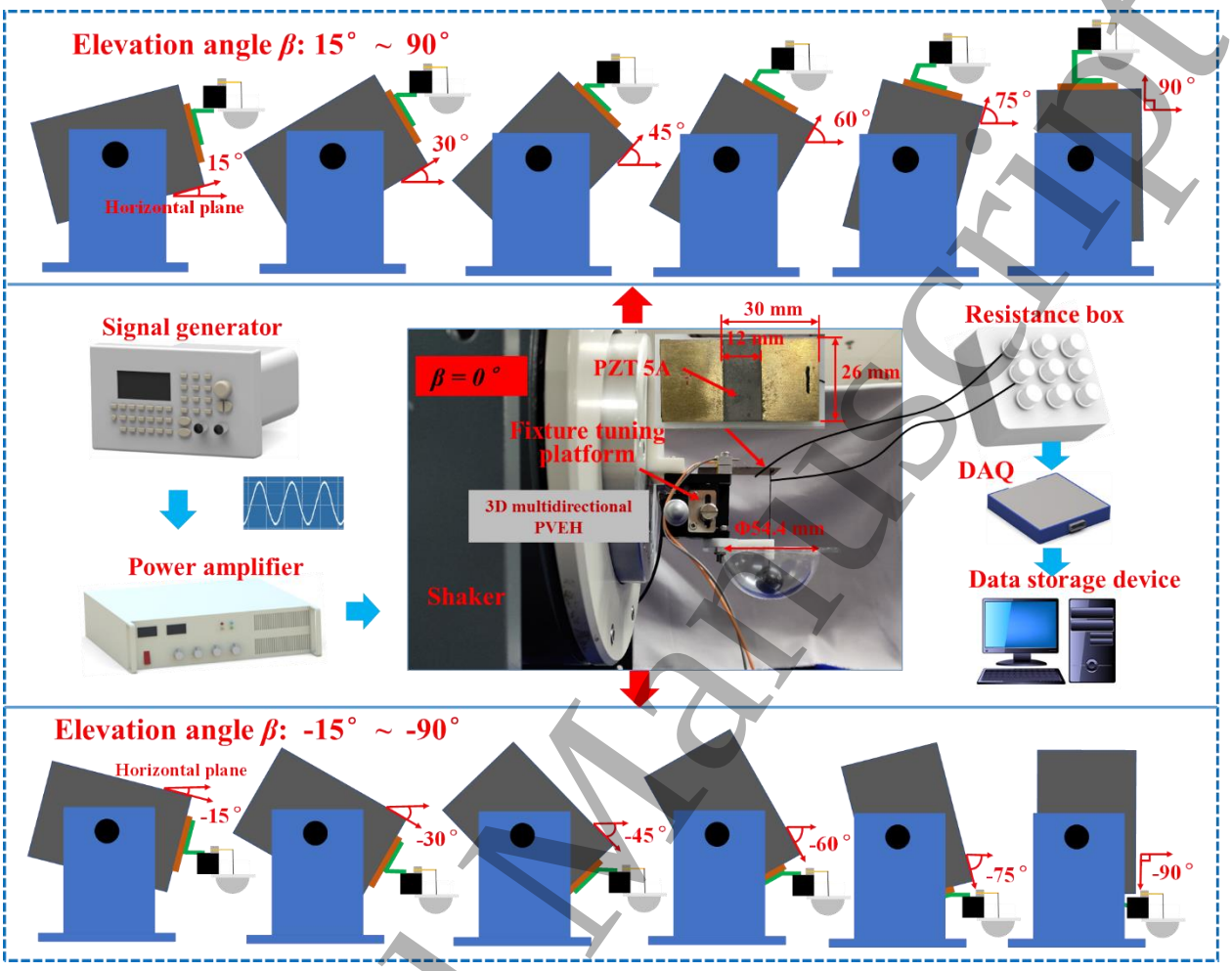

Figure 9. Test Setup for the 3D multidirectional PVEH.

4. Results and Discussion

A series of experiments were conducted to characterize the multidirectional energy harvesting performance of the proposed PVEH in the 3D space under excitation acceleration a in a range of 0.001 g – 0.04 g. Here, g = 9.8 m/s^2 denotes the gravitational acceleration. Frequency upward sweep is performed in the range of 2 Hz – 10 Hz. The rope redundancy δ, which is defined as rope length minus the length of AC (Fig. 1), is varied in the range of 0.3 mm – 0.7 mm. β is varied in the range of -90º – 90º, φ in the range of 0º–360º, and ball mass in the range of 10 grams – 46 grams. According to the output power of the PVEH across the varying resistive load, it is found that the PVEH has similar load response characteristics shown in Fig. 10, where the quasi-optimal resistive load given different accelerations, rope redundancies and elevation angles are 300 kΩ and will be kept at this value for the further characterization of the frequency responses of

the proposed PVEH in the following sections.

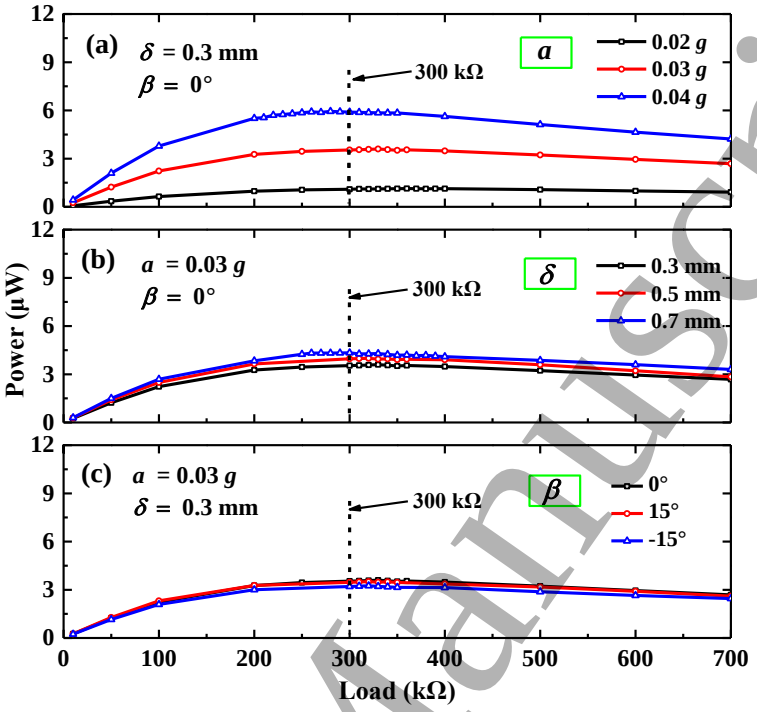

Figure 10. Output powers of the PVEH with varying resistive load given (a) various acceleration a in the range of 0.02 g – 0.04 g, (b) rope redundancy δ in the range of 0.3 mm – 0.7 mm and (c) elevation angle β in the range of -15°– 15°.

4.1 Effects of Acceleration, Rope redundancy and Ball mass

Here, we mainly focus on the effects of excitation acceleration a, rope redundancy δ and ball mass M on the working frequency range and output by experiment and simulation. Because the output RMS voltage is proportional to RMS displacement, the output RMS voltage of the piezoelectric beam can be used as another evaluation parameter for the performance of the proposed PVEH during the experiment. In the simulation, the rope stiffness k_0 is set as 5000 N/m, and other parameters are shown in Table 4. As shown in Figs. 11-13, both experimental and simulation results show that the performance of the proposed PVEH is affected by acceleration, rope redundancy and ball mass. Fig. 11 depicts the experimental and simulation results of frequency responses of the PVEH for various accelerations with β in a range of -30° to 30° and δ = 0.7 mm. The ball mass is 45.9 grams. The figures show that the larger the acceleration, the wider the working frequency and the higher output. Fig. 12 shows the experimental and simulation results of frequency responses of the PVEH for various rope redundancies with β in a range of -30° – 30° and a = 0.04 g. The results show that the working frequency range of the PVEH can be changed

by rope redundancy. Taking $\beta = 30°$, $a = 0.04\ g$ as an example (case 2 in Fig. 12(a)), when the rope redundancy changes from 0.5 mm to 0.7 mm, the working frequency range can be tuned from (2.6 Hz – 8 Hz) to (2.2 Hz – 7.2 Hz).

In addition, the effect of the ball mass on the characteristics of the PVEH was also studied. Fig. 13 describes the experimental and simulation results of frequency responses of the PVEH for various ball masses with β in a range of 0° – 60°. It is found that the increase in ball mass is beneficial for higher output and wider working frequency range since the heavier ball can absorb more mechanical energy from the vibration source. Meanwhile, the tunable performance of the proposed PVEH can be achieved by controlling rope redundancy or ball mass, which will be great helpful for designing. The differences of the simulation and experimental results in working frequency range under different parameters are may attributed to part of mechanical energy ignored as the ball pulling the beam using the rope through the catheter, and geometric approximation with small rolling angle used during modeling building.

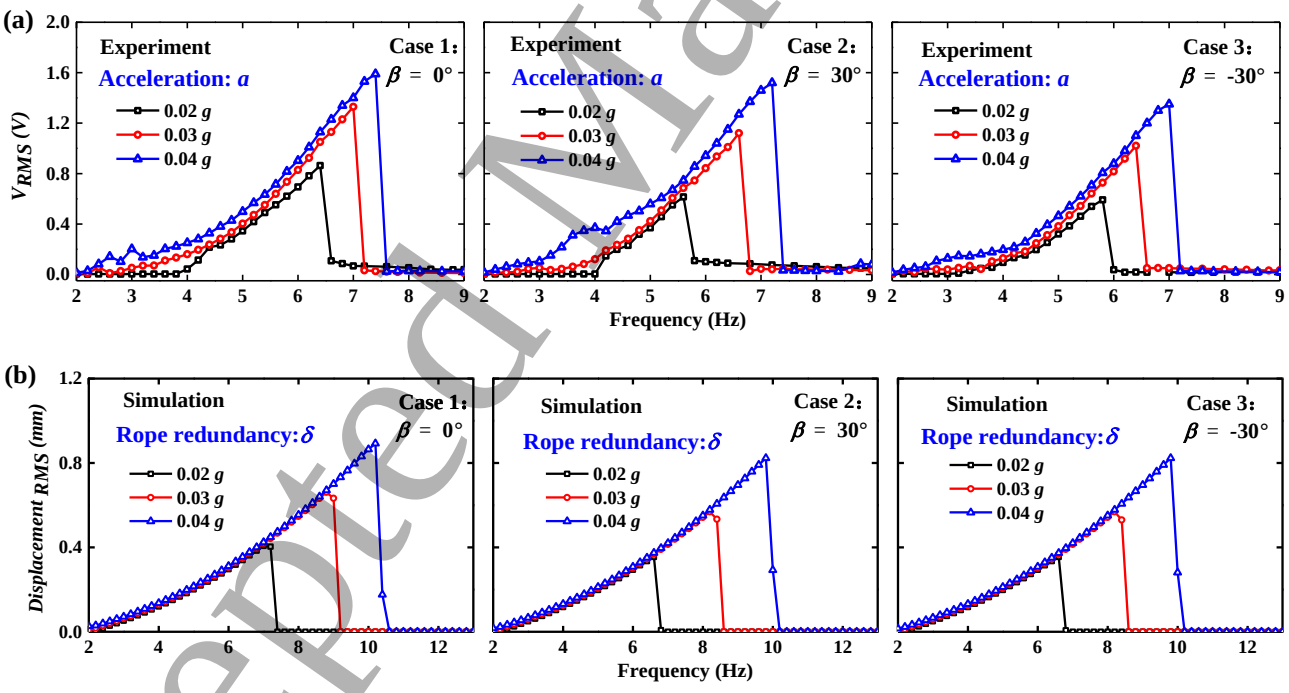

Figure 11. (a) Experimental and simulation (b) results of frequency responses of the 3D multidirectional PVEH for various accelerations with β in a range of -30° – 30° and $\delta = 0.7$ mm.

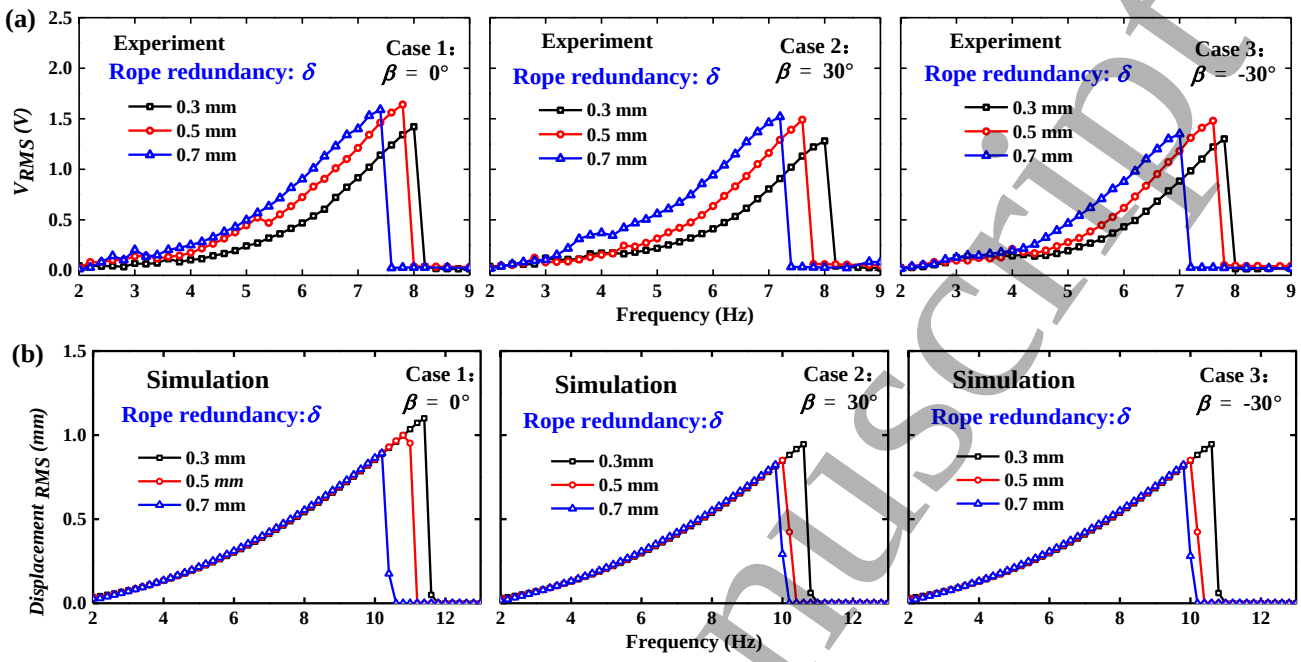

Figure 12. (a) Experimental and simulation (b) results of frequency responses of the 3D multidirectional PVEH for various rope redundancies with β in a range of -30° – 30° and a = 0.04 g.

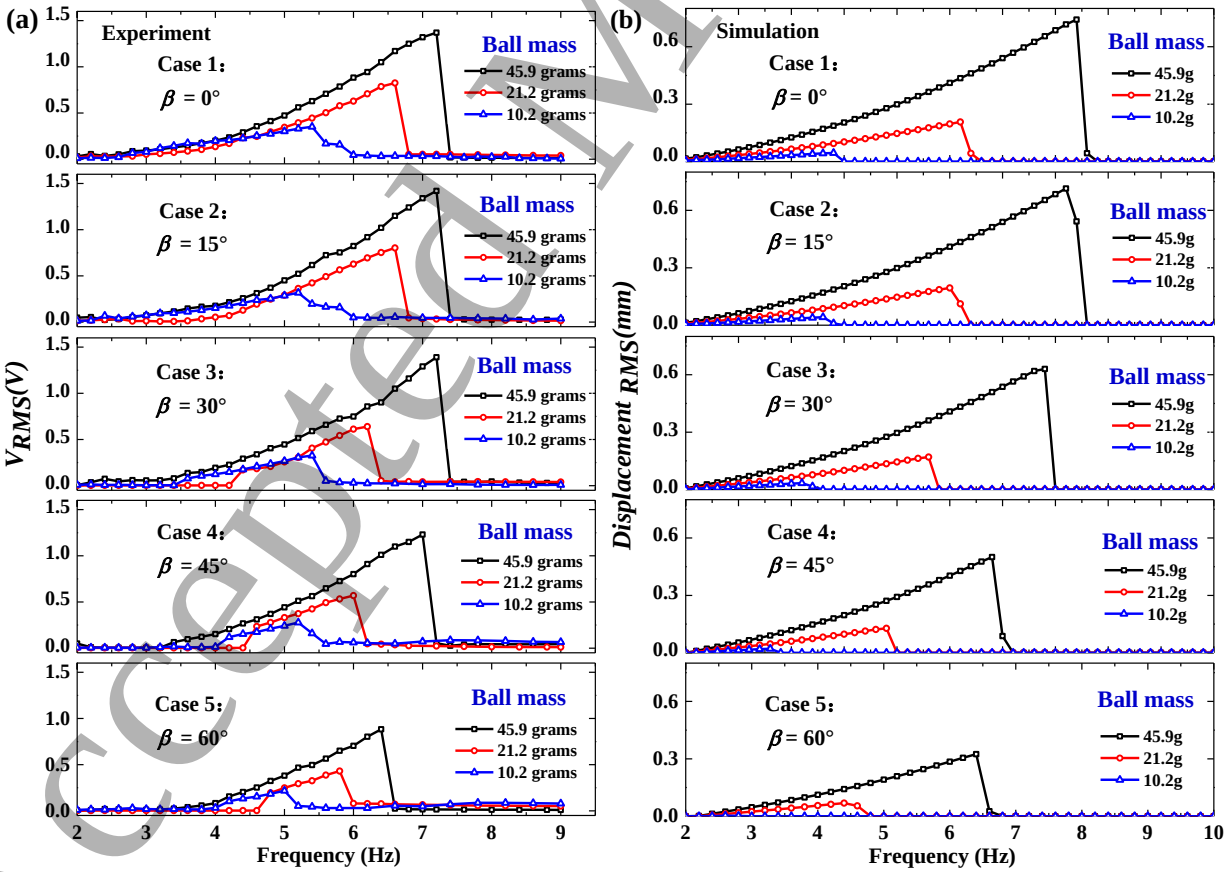

Figure 13. (a) Experimental and simulation (b) results of frequency responses of the 3D

multidirectional PVEH for various ball masses with β in a range of 0° – 60°, a = 0.03 g and δ = 0.5 mm.

4.2 Multidirectional Energy Harvesting in 3D space

When β is unchanged, due to the symmetry of the sphere, it is easy to understand that the PVEH would have consistent performance as φ various in a range of 0° – 360°, which is confirmed in the experiment. With β = 0°, 30° and -30° as examples, Figs. 14 (a) – (c) show that the PVEH have similar frequency responses under various φ. Meanwhile, jump-down phenomena is observed during the frequency upward sweep, which is similar to the hardening configuration with piecewise-linear stiffness induced by stopper impact [29,55–58]. The variation of the output voltage of the PVEH with angles φ depicted in Figs. 14 (d) – (f) show that the PVEH has good symmetry. The slight deviation of output V_{RMS} under different φ is mainly due to the measurement error caused by the device assembly during the experiment. To quantitatively characterise the multidirectional energy harvesting performance of the prototype, the angle bandwidth [50] (the range of angle β corresponding to the output of the PVEH $> 1/\sqrt{2}\ V_{\max}$) was used to evaluate the PVEH's performance under excitations in multiple directions. Results show that the PVEH has an angle bandwidth of 360° due to the symmetry, as shown in Figs. 14 (g) – (i).

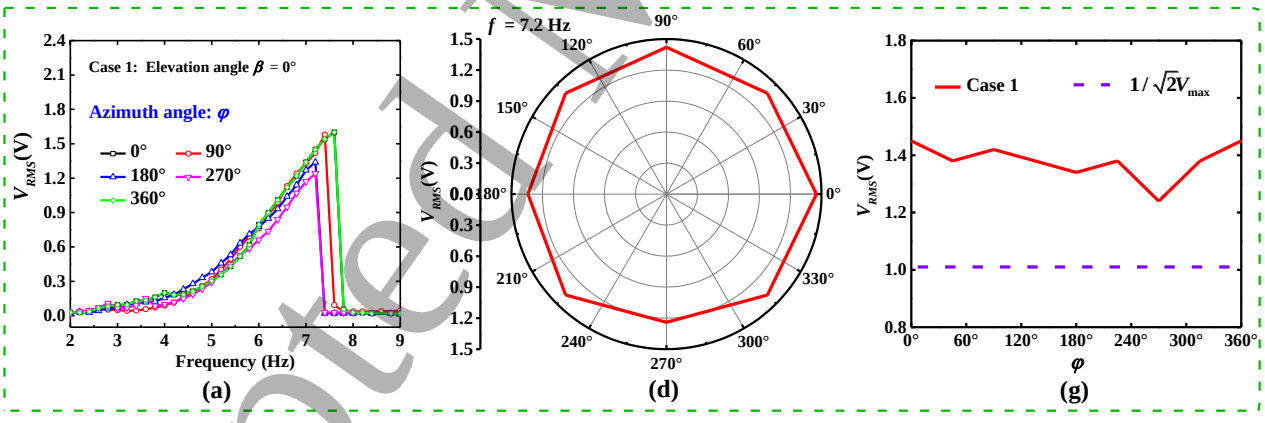

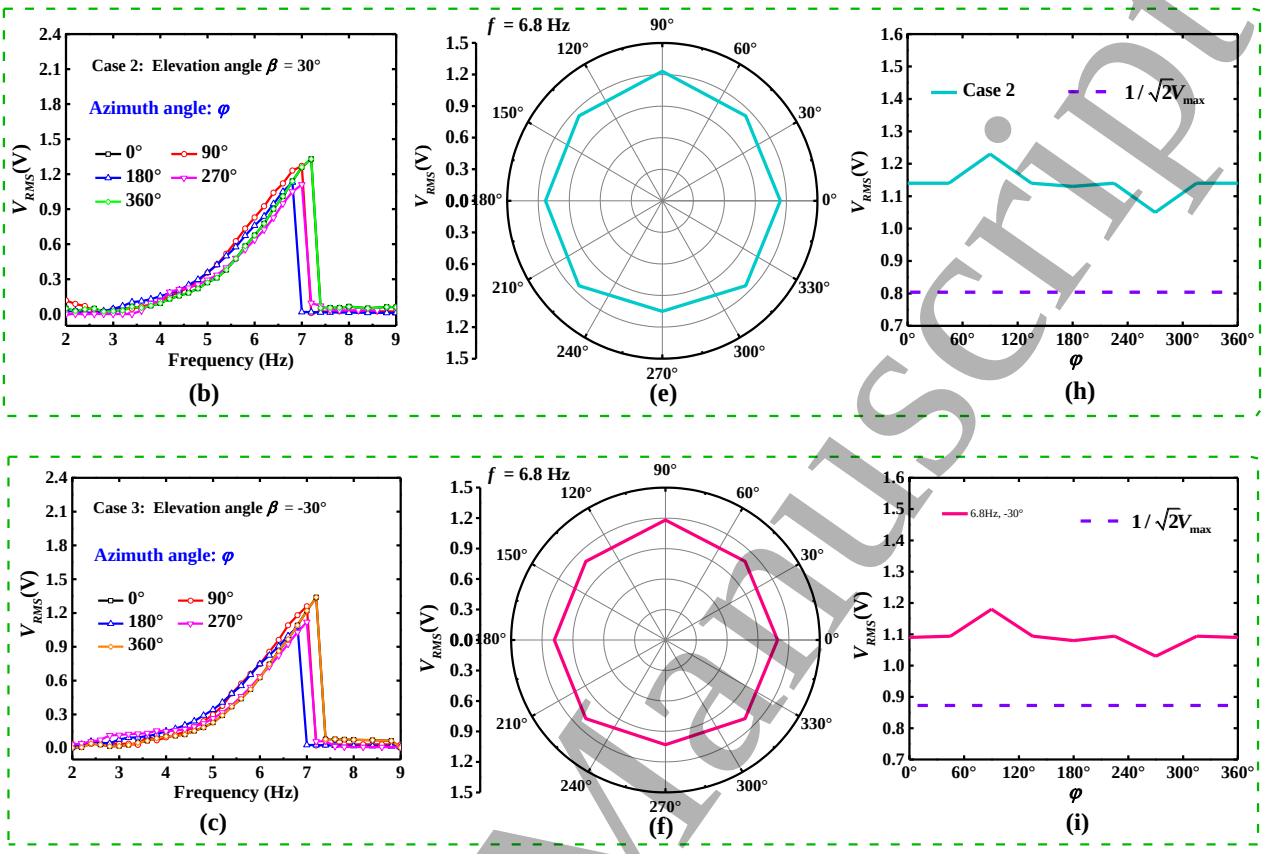

Figure 14. Voltage frequency responses of the PVEH for various φ and β with acceleration a = 0.03 g and rope redundancy δ = 0.5 mm: (a) case1: β = 0°; (b) case2: β = 30°; (c) case3: β = -30°.

The variation of the output voltage of the PVEH with angles φ: (d) case1: β = 0°; (e) case2: β = 30°; (f) case3: β = -30°.

Angle bandwidth of the PVEH: (g) case1: β = 0°; (h) case2: β = 30°; (i) case3: β = -30°.

As β changes from -90° to 90°, the PVEH has output as excitation frequencies in a range of 2 Hz – 9 Hz under ultralow excitations of 0.03 g and 0.04 g, which means the proposed PVEH can capture energy in multiple directions in 3D space. The output is related to the elevation angle β, which can be seen from four cases (1, 2, 3 and 4) shown in Figs. 15 (a) – (d). To describe the multidirectional performance of the PVEH more intuitively, Figs. 15 (e) – (h) depict the variation of the PVEH's voltage with angles β of four cases, where the output voltage of the PVEH measured in a range of -90° – 90° can be extended to 360° due to the symmetry of the structure along the vertical. It can be seen that the proposed PVEH has good symmetry about horizontal (β = 0°) under a low amplitude (< 0.04 g) and low frequency (< 10 Hz) excitation. Meanwhile, as shown in Figs. 15 (i) – (l), the angle bandwidths (output $> 1/\sqrt{2}\ V_{max}$ as the reference) of the prototype can reach

180°, 180°, 240° and 240° respectively. Overall, based on the experiment results mentioned above, the proposed PVEH can realize energy harvesting with multiple directions in 3D space under an ultralow intensity and low frequency excitation vibration.

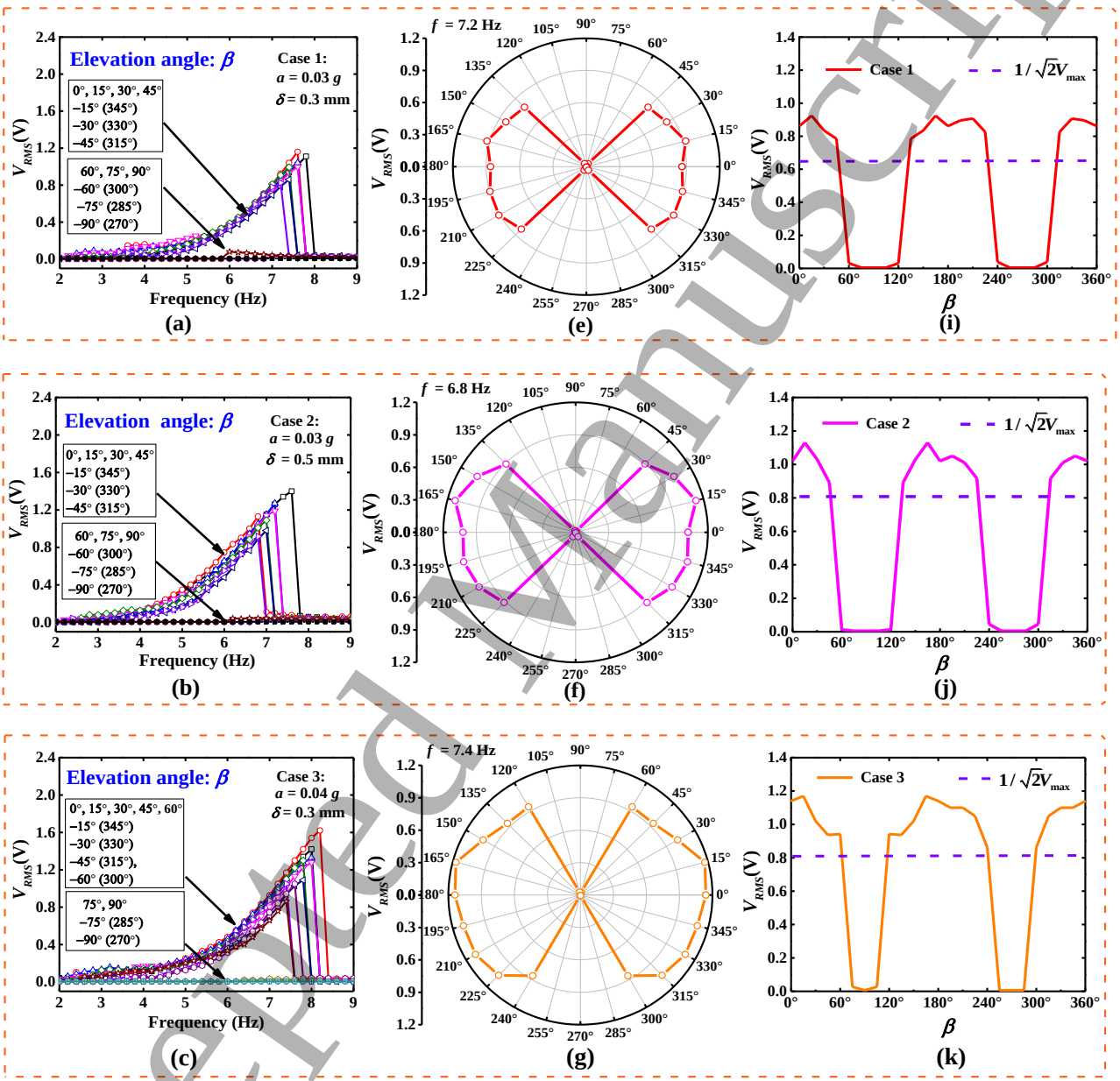

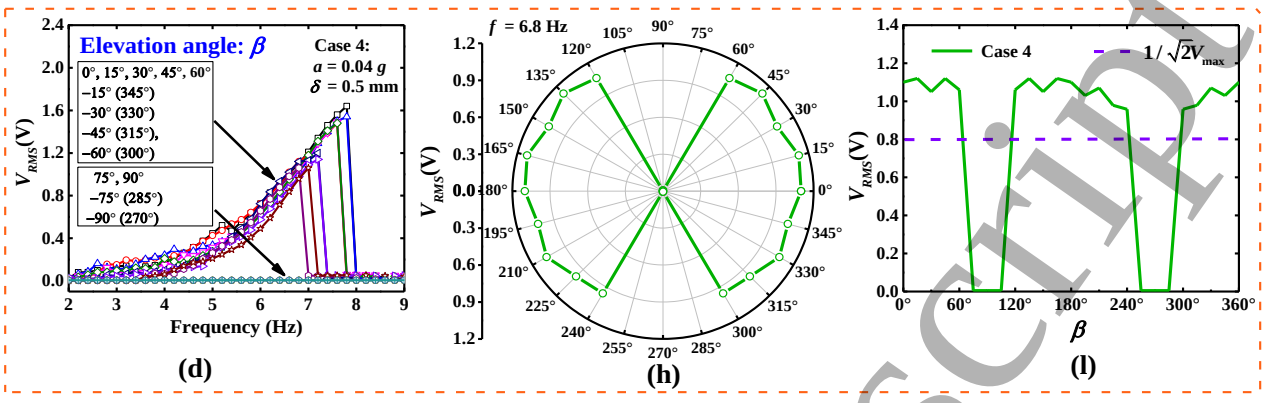

Figure 15. Voltage frequency responses of the PVEH for various β with different acceleration a and rope redundancy δ (a) case 1:a = 0.03 g, δ = 0.3 mm; (b) case 2: a = 0.03 g, δ = 0.5 mm; (c) case 3: a = 0.04 g, δ = 0.3 mm; (d) case 4: a = 0.04 g, δ = 0.5 mm.
The variation of the output voltage of the PVEH with angles β: (e) case 1: f = 7.2 Hz, a = 0.03 g, δ = 0.3 mm; (f) case 2: f = 6.8 Hz, a = 0.03 g, δ = 0.5 mm; (g) case 3: f = 7.4 Hz, a = 0.04 g, δ = 0.3 mm; (h) case 4: f = 6.8 Hz, a = 0.04 g, δ = 0.5 mm.
Angle bandwidth of the PVEH: (i) case 1: f = 7.2 Hz, a = 0.03 g, δ = 0.3 mm; (j) case 2: f = 6.8 Hz, a = 0.03 g, δ = 0.5 mm; (k) case 3: f = 7.4 Hz, a = 0.04 g, δ = 0.3 mm; (l) case 4: f = 6.8 Hz, a = 0.04 g, δ = 0.5 mm.

Furthermore, the output power of the proposed PVEH reaches the level of microwatts (9.0 μW), when its RMS voltage is 1.64 V as shown in Fig. 15 (d); however, the vibration acceleration applied to the PVEH was only 0.04 g. It indicates the proposed PVEH can harvest multidirectional energy from weak-intensity-vibration ambient environments, which also could be observed from a very low value of minimum start-up acceleration (around 0.01 g) discussed in Section 4.2. Table 5 summarizes and compares some typical existing reported low frequency multidirectional PVEHs with our proposed 3D multidirectional PVEH in terms of normalized power density. The volume of the proposed prototype is approximately equal to the half volume of the spherical shell with a radius of 27.2 mm. From Table 5, it can be seen that the performance of the proposed PVEH under various directions with a single piezoelectric cantilever beam were better than those of most PVEHs with multiple generating beams [13,41] under low frequency and ultralow intensity vibration environments. Meanwhile, compared with the proposed PVEH, most multidirectional PVEHs in 3D space had difficulty achieving vibration energy harvesting under excitation with low frequency (< 10 Hz) and low intensity (< 0.1 g) simultaneously. Additionally, the proposed PVEH shows advantages in terms of normalized power density compared with the existing multidirectional PVEHs, and its normalized power density can reach 22.63 μW/(cm^3g^2Hz) under a low frequency of 7.6 Hz and an ultralow intensity of 0.03 g. Therefore, the proposed PVEH using

shell and ball as a low-frequency energy-capturing resonant medium based on rope-driven mechanism exhibits promising potential for application under low frequency, ultralow intensity and multidirectional vibrations in 3D space.

Table 5. Comparison of the proposed and the existing PVEHs under low frequency, low intensity and multidirectional excitations.

References	Power [b] (μW)	Volume [c] (cm^3)	Acceleration (g)	Frequency (Hz)	Numbers of PZT elements	Power density ($\mu W/(cm^3 g^2 Hz)$)	Excitations (2D/3D)
[52][a]	93	19.2	2	5.2	1	0.23	2D
[34]	963.9	3.12	3	18	2	1.91	2D
[43][a]	180	8.47	1.5	6.5	2	1.45	2D
[59][a]	1001	58.8	0.4	17	4	6.29	2D
[13]	13290	/[d]	0.26	2.03	6	/	2D
[60]	5.2	/[d]	0.08	24.5	2	/	2D
[54]	9.8	471.24	0.03	2.6	1	8.89	2D
[51]	22300	/[d]	1.0	14	3	/	2D
[41]	198	/[d]	0.014	22	13	/	3D
[42]	31.8	/[d]	0.6	33	3	/	3D
[47]	330.8	11	0.5	16	1	7.52	3D
This work	9.0	42	0.04	7.8	1	17.17	3D
This work	6.5	42	0.03	7.6	1	22.63	3D

[a] Piezoelectric-electromagnetic hybrid vibration energy harvesters with only the piezoelectric output calculated.

[b] Total output power of all PZT elements.

[c] Space demanded by the energy harvester during motions.

[d] Volume of the device itself is not available.

4.3 Ultralow Start-up Acceleration

As mentioned above, the proposed PVEH can harvest energy efficiently under an ultralow intensity of 0.03 g. In fact, when the acceleration further decreases to 0.01 g, it was found that the PVEH can still have electricity output, indicating that proposed PVEH has a very low value of minimum start-up acceleration. Here, the minimum acceleration required for start-up is defined a_{min} where a load voltage in the level of mV can be observed during the frequency upward sweep (4 Hz – 10 Hz). Furthermore, the minimum start-up acceleration of the PVEH under various β was measured in experiments, as shown in Fig. 16. It can be observed that a_{min} increases with the elevation angle β.

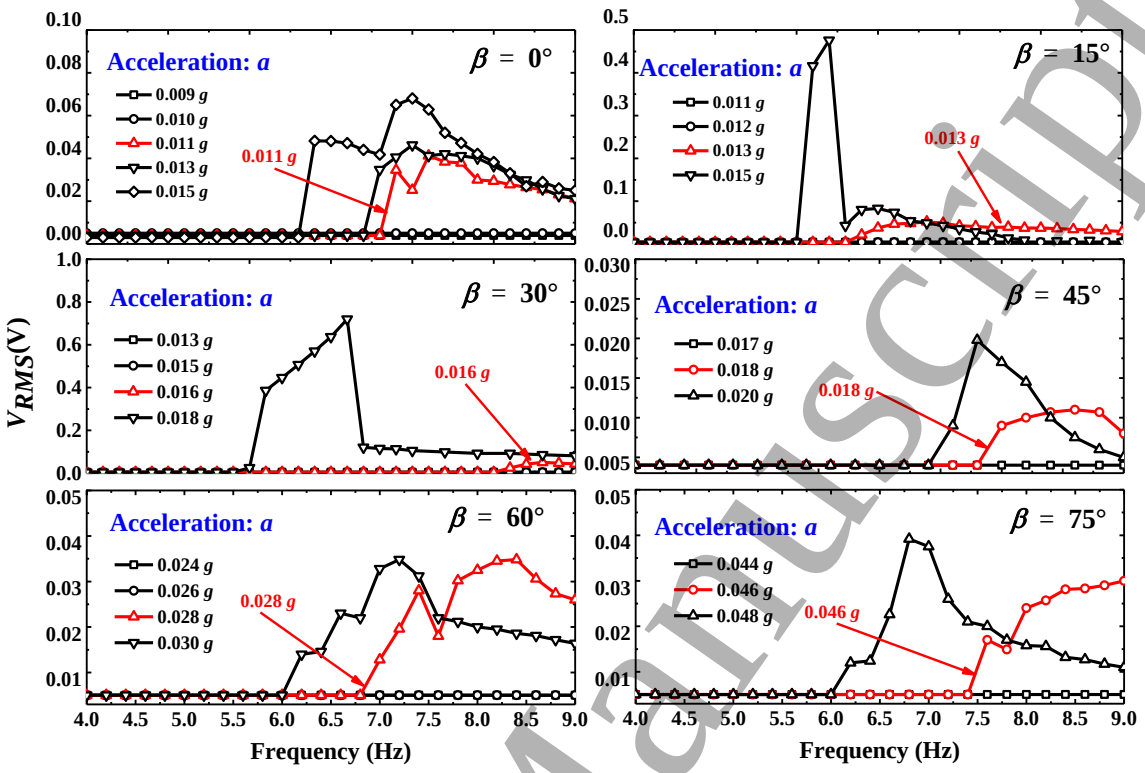

Figure 16. Voltage frequency responses of the PVEH under various accelerations with β in a range of 0° –75°.

To understand the dependence of a_{min} on β ($\neq \pm 90°$), a static force analysis on the minimum acceleration ($a_{\text{min-static}}$) to overcome the friction was conducted as shown in Fig. 17, where $F = ma_{\text{min-static}}$, is the inertial force, and m is the ball mass. F_{N} is the supporting force from the shell. $f_{\text{static}}=\mu F_{\text{N}}$, is the friction, and μ is the static friction coefficient between the ball and shell. Finally, it was found that $a_{\text{min-static}}$ for different β can be expressed by

$$a_{\text{min-static}}(\beta) = \frac{a_{\text{min-static}}(0°)}{\frac{a_{\text{min-static}}(0°)}{g}\sin\beta + \cos\beta} \tag{18}$$

where $a_{\text{min-static}}(0°) = \mu g$.

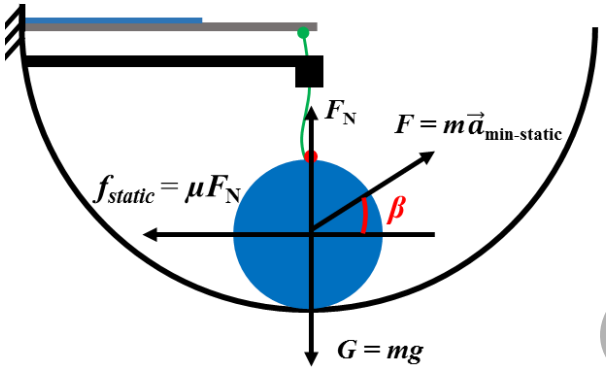

Figure 17. Schematic of static force analysis of the proposed PVEH.

Taking a reference of the relation between $a_{min\text{-}static}$ (β) and $a_{min\text{-}static}$ (0°), if the Eq. (18) is adopted to predict the depends of a_{min} on β, interestingly, it was found that the theoretical a_{min} agree with the experimental a_{min} shown in Fig. 18. This is mainly attributed to the fact that due to a very small rope redundancy ($\delta = 0.5$ mm) adopted in the experiment, it is highly possible to cause the output of the PVEH once the ball overcomes the friction to move.

$$a_{min}(\beta) = \frac{a_{min}(0°)}{\frac{a_{min}(0°)}{g}\sin\beta + \cos\beta} \tag{19}$$

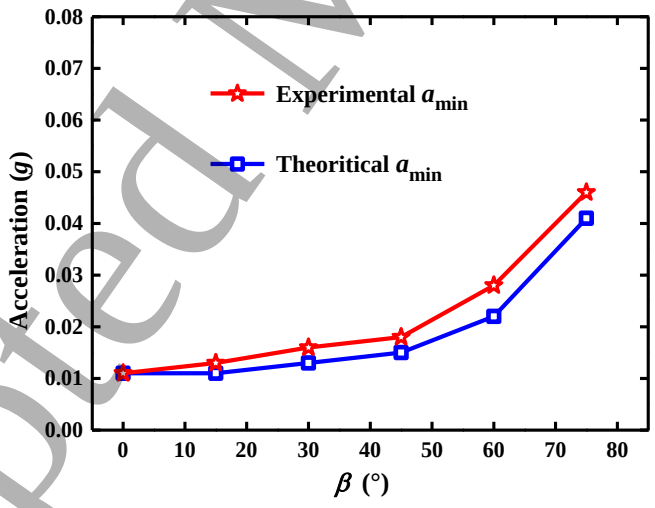

Figure 18. Comparison of the theoretical and experimental results of a_{min} with different β.

5. Conclusions

This paper reports a novel 3D multidirectional PVEH based on a rope-driven mechanism for harvesting energy from low frequency, ultralow intensity and multidirectional vibrations. This is achieved by a low-frequency energy-capturing resonant system formed by a rolling ball in a

hemispherical shell. A prototype is designed, fabricated and experimentally tested to demonstrate the characteristics of the PVEH. The experimental results illustrate that this device can simultaneously achieve low frequency (<10 Hz), ultralow intensity (≤ 0.04 *g*), and multidirectional vibration energy harvesting in 3D space. The PVEH with only one beam demonstrated a good angle bandwidth with 360° for φ and 240° for β under excitation of a = 0.04 g, f = 6.8 Hz. The PVEH can generate an output power of 6.5 μW under a low frequency (7.6 Hz) and an ultralow intensity vibration excitation (0.03 *g*), and the normalized power density can reach 22.63 μW/(cm^3*g*^{2}Hz), which is favourable compared with the existing multidirectional PVEHs. Moreover, the minimum start-up acceleration analysis shows that the developed PVEH can realize energy harvesting under an acceleration as low as 0.01 *g*. In addition, both the simulation and experimental results show that the performance of PVEH can be changed efficiently by tuning the rope redundancy and ball mass. These results unveil and affirm the potential of the proposed PVEH for powering wireless sensors distributed in the low-frequency, low-intensity and 3D-multidirectional vibration environment.

Declaration of Competing Interest

The authors declare that they have no known competing financial interests or personal relationships that could have appeared to influence the work reported in this paper.

Acknowledgements

This work was supported by the National Natural Science Foundation of China (Grant No: 51775465, 52005423), China Postdoctoral Science Foundation (Grant No: 2020M671946) and Knowledge Innovation Program of Shenzhen City (Fundamental Research, Free Exploration) (Grant No: JCY20190809162001746).

References

[1] Y. Li, D. Yin, X. Cheng, J. Chen, A. Zhou, X. Ji, Y. Li, Vibration energy harvesting with piezoelectric ceramics working in d_{33} mode by using a spring-mass-spring oscillator, J. Appl. Phys. 127 (2020) 0–8. https://doi.org/10.1063/1.5116554.

[2] Y. Zhang, A. Luo, Y. Wang, X. Dai, Y. Lu, F. Wang, Rotational electromagnetic energy harvester for human motion application at low frequency rotational electromagnetic energy harvester for human motion application at low frequency, Appl. Phys. Lett. 116 (2020) 053902.

https://doi.org/10.1063/1.5142575.

[3] B. Yang, Z. Yi, G. Tang, J. Liu, A gullwing-structured piezoelectric rotational energy harvester for low frequency energy scavenging, Appl. Phys. Lett. 115 (2019) 063901. https://doi.org/10.1063/1.5110368.

[4] W. Wang, J. Cao, C. Bowen, S. Zhou, J. Lin, Optimum resistance analysis and experimental veri fi cation of nonlinear piezoelectric energy harvesting from human motions, Energy. 118 (2017) 221–230. https://doi.org/10.1016/j.energy.2016.12.035.

[5] S. Zhou, J. Cao, D. Inman, J. Lin, S. Liu, Z. Wang, Broadband tristable energy harvester: Modeling and experiment verification, Appl. Energy. 133 (2014) 33–39. https://doi.org/10.1016/j.apenergy.2014.07.077.

[6] J. Cao, W. Wang, S. Zhou, D. Inman, J. Lin, Nonlinear time-varying potential bistable energy harvesting from human motion, Appl. Phys. Lett. 107 (2015) 143904. https://doi.org/10.1063/1.4932947.

[7] H. Liu, S. Zhang, R. Kathiresan, T. Kobayashi, C. Lee, Development of piezoelectric microcantilever flow sensor with wind-driven energy harvesting capability, Appl. Phys. Lett. 100 (2012) 223905. https://doi.org/10.1063/1.4723846.

[8] T. Yildirim, M. Ghayesh, W. Li, G. Alici, A review on performance enhancement techniques for ambient vibration energy harvesters, Renew. Sustain. Energy Rev. 71 (2017) 435–449. https://doi.org/10.1016/j.rser.2016.12.073.

[9] K. Fan, J. Chang, F. Chao, W. Pedrycz, Design and development of a multipurpose piezoelectric energy harvester, Energy Convers. Manag. 96 (2015) 430–439. https://doi.org/10.1016/j.enconman.2015.03.014.

[10] L. Van Blarigan, P. Danzl, J. Moehlis, A broadband vibrational energy harvester, Appl. Phys. Lett. 100 (2012) 253904. https://doi.org/10.1063/1.4729875.

[11] H. Li, C. Tian, Z. Deng, Energy harvesting from low frequency applications using piezoelectric materials, Appl. Phys. Rev. 1 (2014) 041301. https://doi.org/10.1063/1.4900845.

[12] H. Fu, S. Theodossiades, B. Gunn, I. Abdallah, E. Chatzi, Ultra-low frequency energy harvesting using bi-stability and rotary-translational motion in a magnet-tethered oscillator, Nonlinear Dyn. 101 (2020) 2131–2143. https://doi.org/10.1007/s11071-020-05889-9.

[13] Y. Wu, J. Qiu, S. Zhou, H. Ji, Y. Chen, S. Li, A piezoelectric spring pendulum oscillator used for multi-directional and ultra-low frequency vibration energy harvesting, Appl. Energy. 231 (2018) 600–614. https://doi.org/10.1016/j.apenergy.2018.09.082.

[14] L. Gu, C. Livermore, Impact-driven, frequency up-converting coupled vibration energy harvesting device for low frequency operation, Smart Mater. Struct. 20 (2011) 045004. https://doi.org/10.1088/0964-1726/20/4/045004.

[15] K. Kwok, P. Hitchcock, M. Burton, Perception of vibration and occupant comfort in wind-excited tall buildings, J. Wind Eng. Ind. Aerodyn. 97 (2009) 368–380. https://doi.org/10.1016/j.jweia.2009.05.006.

[16] H. Le, E.-S. Hwang, Investigation of deflection and vibration criteria for road bridges, KSCE J. Civ. Eng. 21 (2017) 829–837. https://doi.org/10.1007/s12205-016-0532-3.

[17] N. Li, Studies on vibration control of offshore platforms under random wave loads, Ocean University of China, 2011. https://doi.org/10.7666/d.y2212726.

[18] S. Roundy, P. Wright, J. Rabaey, A study of low level vibrations as a power source for wireless sensor nodes, Comput. Commun. 26 (2003) 1131–1144. https://doi.org/10.1016/S0140-3664(02)00248-7.

[19] R.M. Toyabur, M. Salauddin, J.Y. Park, Design and experiment of piezoelectric multimodal energy harvester for low frequency vibration, Ceram. Int. 43 (2017) S675–S681. https://doi.org/10.1016/j.ceramint.2017.05.257.

[20] L. Xie, S. Cai, G. Huang, L. Huang, J. Li, X. Li, On Energy Harvesting From a Vehicle Damper, IEEE/ASME Trans. Mechatronics. 25 (2020) 108–117. https://doi.org/10.1109/TMECH.2019.2950952.

[21] W. Wei, Influence and analysis of urban road traffic loads on neighboring buildings, Wuhan University

Of Technology, 2019.

[22] Z. Lin, Y. Zhang, Dynamics of a mechanical frequency up-converted device for wave energy harvesting, J. Sound Vib. 367 (2016) 170–184. https://doi.org/10.1016/j.jsv.2015.12.048.

[23] H. Wang, B. Li, Y. Liu, W. Zhao, Low-frequency, broadband piezoelectric vibration energy harvester with folded trapezoidal beam, Rev. Sci. Instrum. 90 (2019) 035001. https://doi.org/10.1063/1.5034495.

[24] H. Liu, C. Lee, T. Kobayashi, C.J. Tay, C. Quan, A new S-shaped MEMS PZT cantilever for energy harvesting from low frequency vibrations below 30 Hz, Microsyst. Technol. 18 (2012) 497–506. https://doi.org/10.1007/s00542-012-1424-1.

[25] Y. Tian, G. Li, Z. Yi, J. Liu, B. Yang, A low-frequency MEMS piezoelectric energy harvester with a rectangular hole based on bulk PZT film, J. Phys. Chem. Solids. 117 (2018) 21–27. https://doi.org/10.1016/j.jpcs.2018.02.024.

[26] N. Jackson, O.Z. Olszewski, C. O'Murchu, A. Mathewson, Ultralow-frequency PiezoMEMS energy harvester using thin-film silicon and parylene substrates, J. Micro/ Nanolithography, MEMS, MOEMS. 17 (2018) 1. https://doi.org/10.1117/1.jmm.17.1.015005.

[27] K. Rashmi, A. Rao, A. Jayarama, R. Pinto, Low frequency piezoelectric P(VDF-TrFE) micro-cantilevers with a novel MEMS process for vibration sensor and energy harvester applications, Smart Mater. Struct. 28 (2019). https://doi.org/10.1088/1361-665X/ab19d2.

[28] M. Halim, S. Khym, J. Park, Frequency up-converted wide bandwidth piezoelectric energy harvester using mechanical impact, J. Appl. Phys. 114 (2013) 044902-5. https://doi.org/10.1063/1.4816249.

[29] H. Liu, C. Lee, T. Kobayashi, C. Tay, C. Quan, Investigation of a MEMS piezoelectric energy harvester system with a frequency-widened-bandwidth mechanism introduced by mechanical stoppers, Smart Mater. Struct. 21 (2012). https://doi.org/10.1088/0964-1726/21/3/035005.

[30] M. Halim, J. Park, Theoretical modeling and analysis of mechanical impact driven and frequency up-converted piezoelectric energy harvester for low-frequency and wide-bandwidth operation, Sensors Actuators, A Phys. 208 (2014) 56–65. https://doi.org/10.1016/j.sna.2013.12.033.

[31] K. Vijayan, M.I. Friswell, H. Haddad Khodaparast, S. Adhikari, Non-linear energy harvesting from coupled impacting beams, Int. J. Mech. Sci. 96–97 (2015) 101–109. https://doi.org/10.1016/j.ijmecsci.2015.03.001.

[32] J. Zhang, L. Kong, L. Zhang, F. Li, W. Zhou, S. Ma, L. Qin, A novel ropes-driven wideband piezoelectric vibration energy harvester, Appl. Sci. 6 (2016) 1–13. https://doi.org/10.3390/app6120402.

[33] J. Zhang, L. Qin, A tunable frequency up-conversion wideband piezoelectric vibration energy harvester for low-frequency variable environment using a novel impact- and rope-driven hybrid mechanism, Appl. Energy. 240 (2019) 26–34. https://doi.org/10.1016/j.apenergy.2019.01.261.

[34] S. Ju, C. Ji, Impact-based piezoelectric vibration energy harvester, Appl. Energy. 214 (2018) 139–151. https://doi.org/https://doi.org/10.1016/j.apenergy.2018.01.076.

[35] N. Tran, M.H. Ghayesh, M. Arjomandi, A review on nonlinear techniques for performance enhancement, Int. J. Eng. Sci. 127 (2018) 435–449. https://doi.org/10.1016/j.ijengsci.2018.02.003.

[36] Q. Tang, X. Li, Two-stage wideband energy harvester driven by multimode coupled vibration, IEEE/ASME Trans. Mechatronics. 20 (2015) 115–121. https://doi.org/10.1109/TMECH.2013.2296776.

[37] A. Wickenheiser, E. Garcia, Broadband vibration-based energy harvesting improvement through frequency up-conversion by magnetic excitation, Smart Mater. Struct. 19 (2010) 1–11. https://doi.org/10.1088/0964-1726/19/6/065020.

[38] Q. Tang, Y. Yang, X. Li, Bi-stable frequency up-conversion piezoelectric energy harvester driven by non-contact magnetic repulsion, Smart Mater. Struct. 20 (2011) 1–6. https://doi.org/10.1088/0964-1726/20/12/125011.

[39] P. Pillatsch, E.M. Yeatman, A.S. Holmes, A piezoelectric frequency up-converting energy harvester with

rotating proof mass for human body applications, Sensors Actuators A Phys. 206 (2014) 178–185. https://doi.org/10.1016/j.sna.2013.10.003.

[40] W.-J. Su, J. Zu, An innovative tri-directional broadband piezoelectric energy harvester, Appl. Phys. Lett. 103 (2013) 203901. https://doi.org/10.1063/1.4830371.

[41] R. Chen, L. Ren, H. Xia, X. Yuan, X. Liu, Energy harvesting performance of a dandelion-like multi-directional piezoelectric vibration energy harvester, Sensors Actuators, A Phys. 230 (2015) 1–8. https://doi.org/10.1016/j.sna.2015.03.038.

[42] Q. Yu, J. Yang, X. Yue, A. Yang, J. Zhao, N. Zhao, Y. Wen, P. Li, Nonlinear arbitrary-directional broadband piezoelectric vibration energy harvester using 3-DOF parallel mechanism, AIP Adv. 5 (2015) 047144. https://doi.org/10.1063/1.4919401.

[43] K. Fan, S. Liu, H. Liu, Y. Zhu, W. Wang, D. Zhang, Scavenging energy from ultra-low frequency mechanical excitations through a bi-directional hybrid energy harvester, Appl. Energy. 216 (2018) 8–20. https://doi.org/10.1016/j.apenergy.2018.02.086.

[44] J. Yang, Y. Wen, P. Li, X. Yue, Q. Yu, X. Bai, A two-dimensional broadband vibration energy harvester using magnetoelectric transducer, Appl. Phys. Lett. 103 (2013) 243903. https://doi.org/10.1063/1.4847755.

[45] Z. Lin, J. Chen, X. Li, J. Li, J. Liu, Q. Awais, J. Yang, Broadband and three-dimensional vibration energy harvesting by a non-linear magnetoelectric generator, Appl. Phys. Lett. 109 (2016) 253903. https://doi.org/10.1063/1.4972188.

[46] J. Zhao, J. Yang, Z. Lin, N. Zhao, J. Liu, Y. Wen, P. Li, An arc-shaped piezoelectric generator for multi-directional wind energy harvesting, Sensors Actuators A Phys. 236 (2015) 173–179. https://doi.org/10.1016/j.sna.2015.10.047.

[47] N. Zhao, J. Yang, Q.M. Yu, J.X. Zhao, J. Liu, Y.M. Wen, P. Li, Three-dimensional piezoelectric vibration energy harvester using spiral-shaped beam with triple operating frequencies, Rev. Sci. Instrum. 87 (2016) 015003. https://doi.org/10.1063/1.4940417.

[48] Y. Yang, H. Wu, C.K. Soh, Experiment and modeling of a two-dimensional piezoelectric energy harvester, Smart Mater. Struct. 24 (2015) 125011. https://doi.org/10.1088/0964-1726/24/12/125011.

[49] Y. Zeng, L. Jiang, Y. Sun, Y. Yang, Y. Quan, S. Wei, G. Lu, R. Li, J. Rong, Y. Chen, Q. Zhou, 3D-printing piezoelectric composite with honeycomb structure for ultrasonic devices, Micromachines. 11 (2020) 713. https://doi.org/10.3390/MI11080713.

[50] P. Wang, X. Liu, H. Zhao, W. Zhang, X. Zhang, Y. Zhong, Y. Guo, A two-dimensional energy harvester with radially distributed piezoelectric array for vibration with arbitrary in-plane directions, J. Intell. Mater. Syst. Struct. 30 (2019) 1094–1104. https://doi.org/10.1177/1045389X19828820.

[51] G. Yuan, S. Zhuo, D. Wang, Nonlinear arbitrary-directional broadband piezoelectric vibration energy harvester using 3-DOF parallel mechanism, Smart Mater. Struct. 28 (2019) 085016. https://doi.org/10.1088/1361-665X/ab2491.

[52] M.A. Halim, M.H. Kabir, H. Cho, J.Y. Park, A frequency up-converted hybrid energy harvester using transverse impact-driven piezoelectric bimorph for human-limb motion, Micromachines. 10 (2019) 701. https://doi.org/10.3390/mi10100701.

[53] J. Xu, J. Tang, Multi-directional energy harvesting by piezoelectric cantilever-pendulum with internal resonance, Appl. Phys. Lett. 107 (2015) 213902. https://doi.org/10.1063/1.4936607.

[54] F. Yang, J. Zhang, M. Lin, S. Ouyang, L. Qin, An ultralow frequency, low intensity, and multidirectional piezoelectric vibration energy harvester using liquid as energy-capturing medium, Appl. Phys. Lett. 117 (2020) 173901–7. https://doi.org/10.1063/5.0022881.

[55] M. Daqaq, R. Masana, A. Erturk, D. Dane Quinn, On the role of nonlinearities in vibratory energy harvesting: a critical review and discussion, Appl. Mech. Rev. 66 (2014) 040801-23.

https://doi.org/10.1115/1.4026278.

[56] X. Wang, C. Chen, N. Wang, H. San, Y. Yu, E. Halvorsen, X. Chen, A frequency and bandwidth tunable piezoelectric vibration energy harvester using multiple nonlinear techniques, Appl. Energy. 190 (2017) 368–375. https://doi.org/10.1016/j.apenergy.2016.12.168.

[57] X. Li, K. Liu, L. Xiong, L. Tang, Development and validation of a piecewise linear nonlinear energy sink for vibration suppression and energy harvesting, J. Sound Vib. 503 (2021) 116104. https://doi.org/10.1016/j.jsv.2021.116104.

[58] L. Tang, Y. Yang, C.K. Soh, Toward broadband vibration-based energy harvesting, J. Intell. Mater. Syst. Struct. 21 (2010) 1867–1897. https://doi.org/10.1177/1045389X10390249.

[59] R.M. Toyabur, M. Salauddin, H. Cho, J.Y. Park, A multimodal hybrid energy harvester based on piezoelectric-electromagnetic mechanisms for low-frequency ambient vibrations, Energy Convers. Manag. 168 (2018) 454–466. https://doi.org/10.1016/j.enconman.2018.05.018.

[60] H. Fu, Z. Sharif-Khodaei, F. Aliabadi, A bio-inspired host-parasite structure for broadband vibration energy harvesting from low-frequency random sources, Appl. Phys. Lett. 114 (2019) 143901. https://doi.org/10.1063/1.5092593.